INDIUM PHOSPHIDE DOUBLE HETEROJUNCTION BIPOLAR TRANSISTORS WITH T-SHAPED EMITTER METAL FEATURES HAVING CUTOFF FREQUENCIES IN EXCESS OF 200 GHZ

A.K. Fung, L. Samoska, J. Velebir, P. Siegel
California Institute of Technology-Jet Propulsion Laboratory, Pasadena, CA 91109, USA

M. Rodwell, V. Paidi, Z. Griffith
Department of Electrical and Computer Engineering, University of California, Santa Barbara, CA 93106, USA

R. Malik
RJM Semiconductor, Berkeley Heights, NJ 07922, USA

Abstract

We demonstrate Indium Phosphide Double Heterojunction Bipolar Transistors (DHBTs) with simultaneous power gain cutoff frequency Fmax of 288 GHz and current gain cutoff frequency Ft of 251 GHz. The microfabrication procedure we implement differ from most DHBT processes in that T-shaped emitter features are utilized to improve functional yield, and for performance and reliability considerations. We report on our DHBT process, and the electrical characteristics of transistor and matched DHBT amplifiers fabricated in it.

Motivation and Background

Instruments for determining the chemical composition and time evolution of stellar objects and Earth's atmosphere often do so through observations of the electromagnetic spectrum emanating from these sources. The method of molecular spectroscopy through heterodyne remote sensing utilizes local oscillator (LO) sources up to terahertz frequencies (1,2). These LOs utilize amplifiers to increase the output power of the oscillator chain. Our primary purpose is to develop advanced transistor technology to enable higher frequency power amplifiers for progressing local oscillator chain performance. Additionally, an advanced high speed and high power transistor technology can be used to improve other electronic systems by providing greater communication bandwidth, higher radar resolution, and/or faster signal processing speeds (see for more examples (3,4)).

Indium phosphide (InP) heterojunction bipolar transistors (HBTs) are well suited for both high speed and high output power operation, because of the ability to tailor the material in each physical region of electron transport for optimizing performance. InP HBTs can be grown with an alloy or doping graded base region to create a built in electric field to increase electron transport velocity through the transistor. Also a high-electric-field-breakdown material such as InP can be deposited in the collector region of

the transistor so that it may operate at higher voltages while maintaining short electron transport distances for speed. Recent efforts in InP HBTs have produced some of the fastest transistors in the world. Through lateral scaling by undercutting the collector epitaxy, HBTs with Fmax of 687 GHz and Ft of 215 GHz have been reported (5). By vertically scaling in reducing the epitaxial thickness of HBTs, Fmax and Ft of 246 and 604 GHz, respectively, have been demonstrated (6). Simultanous high Fmax and Ft of 505 and 391 GHz, respectively, have also been shown through scaling and minimizing parasitic resistances (7). Ensuing electronics operating at record speeds have been produced. Static frequency dividers clocked at over 150 GHz have been measured (8,9).

InP DHBT T-Emitter Structure

The InP DHBT epitaxial material used in this study is grown by molecular beam epitaxy and consists of a 120 nm InP silicon doped emitter, a 30 nm carbon graded doped InGaAs base layer from $5x10^{19}$ to $8x10^{19}$ cm^{-3}, and a 170nm InP silicon doped collector. Electron beam lithography is used to produce submicron sized emitter stripe widths. Stepper lithography is used in all other patterning steps. Etching is done entirely with wet chemistry and metal deposition with electron beam evaporation. Passivation is made with benzocyclobutene. Gold airbridges are used for interconnects. All other aspects of the process is similar to the conventional triple mesa process discussed elsewhere (see for example ref. 4).

The T-emitter metal feature in this study is produced with a trilayer PMMA/copolymer/PMMA resist stack and electron beam lithography in a metal liftoff process. The T-emitter structure relaxes the requirement of undercut etching of the emitter metal feature, compared to the conventional rectangular emitter structure in a self-aligned base metal process. This is because the T-emitter feature provides in advance the shadow mask spacer for base metal deposition unlike the conventional process that defines the spacer during the emitter metal undercut etch step (see Fig. 1). In the conventional process simultaneous etching of the emitter semiconductor to the base layer and emitter undercut etching to form the base metal spacer is required. In addition we have observed improved functional yield with T-shaped emitters. We attribute this to the spacer the T-emitter provides, such that even in the case of incomplete or uneven etching of the emitter semiconductor material in the vicinity along the periphery of the emitter metal stripe in defining the base metal spacer, the T-emitter still provides for a spacer. Also because the T-emitter allows for wet etching to initiate in the [100] direction during the base-emitter metal spacer formation, the etch has better access to the emitter semiconductor epitaxy to aid etching, in contrast to the conventional process where the spacer etch initiates primarily in the in-plane [011] and [01-1] directions, blocked by the emitter metal. Other advantages of using the T-emitter arises from a thicker allowable base metal that may be deposited compared to the conventional structure (see Fig. 1). Thicker base metal can improve transistor performance by reducing the electrical and thermal resistance, and inductance of the base metal stripe. For reliability considerations, it has been previously reported that emitter stripes with the long dimension aligned in the [01-1] direction are more electrically invariant under thermal-electrical stress tests (10). The cause of this has been attributed to effects related

to the angle that the etched emitter semiconductor layer makes with the base semiconductor layer. The T-emitter structure process proceeds equally well with the emitter stripe aligned in either the [011] or [01-1] orientation, and so in the T-emitter process we aligned the emitter stripe in the [01-1] direction. In contrast, in the conventional self-aligned base metal process the emitter stripes are generally aligned with the long dimension in the [011] direction because the acute angle of the etched emitter material to base layer provides for the spacer between the etched emitter semiconductor layer and the self-aligned base metal that is subsequently deposited, for preventing electrical shorting. Figure 1(a) shows the v-groove emitter profile after emitter etch for the T-emitter structure oriented along the [01-1] direction. The dove-tail profile in the standard emitter structure for an emitter stripe arranged in the [011] direction is shown in Figure 1(b).

InP DHBT Electrical Characteristics

DC electrical characteristics of HBTs show small signal current gain β of approximately 40. Typical common-emitter current-voltage characteristics are shown in Figure 2(a). RF S-parameter measurements are made with an Agilent 8510C vector network analyzer and GGB Industries Inc. coplanar waveguide probes. On-wafer line-reflect-line calibration standards are used to de-embed the DHBT's S-parameters from their coplanar waveguide wiring environment. Mason's unilateral gain U and current gain H21 are calculated from the measured S-parameters as a function of frequency and are displayed in Figure 2(b). A standard –20dB/dec extrapolation based on the behavior of a single pole hybrid-pi model is used to determine Fmax to be 288 GHz and Ft to be 251 GHz, where the extrapolated U and H21 crosses 0 dB gain.

Amplifier designs based on approximated models for the epitaxial layer structure and transistor layout have also been fabricated. Matching and stabilization are done with stub tuning and NiCr resistors (see Fig. 3(a)). RF characterization in W-band (75-110 GHz) is performed with an Agilent 8510C with Oleson Microwave Lab WR-10 waveguide frequency extenders and GGB coplanar waveguide probes. Figure 3(b) shows the measured gain S21 magnitude of a MMIC amplifier. Peak gain S21 is 3.9dB at 82.5 GHz. Performance of initial amplifiers is limited due to the approximate models used prior to the fabrication run.

Conclusion

Advances in transistor technology in speed and output power are needed to advance instruments for NASA remote sensing and commercial/military applications in communications, radar and signal processing. We have developed InP DHBT technology with T-emitter metal features for increasing functional yield, and with the goal of improving performance and reliability of the transistors. DHBTs with Fmax of 288 and Ft of 251 GHz have been demonstrated, and also a prototype MMIC W-band amplifier with peak gain of 3.9 dB at 82.5 GHz. The present generation of DHBTs has cutoff frequencies that are over 100 GHz higher than our previous generation of transistors (11).

Additional scaling in the lateral and vertical dimensions of the transistors is expected to continue to increase performance. Modeling of fabricated transistors for future designs will improve MMIC amplifiers. Studies are required to determine if the T-emitter stripe orientation and benzocyclobutene emitter-base junction coverage for passivation provide adequate reliability for practical applications.

Acknowledgments

The research and development presented in this paper is carrier out at the California Institute of Technology Jet Propulsion Laboratory, a federally funded research and development center under a contract with the MDA under contract DTRA-01-03-C-0033, managed by DTRA. The authors thank Richard Muller and Pierre Echternach at JPL for providing electron beam lithography.

References

1. G. Chattopadhyay, E. Schlecht, J. Ward, J. Gill, H. Javadi, F. Maiwald, and I. Mehdi, IEEE Trans. Microwave Theory Tech., 52, 1538 (2004).
2. A. Maestrini, J. Ward, J. Gill, H. Javadi, E. Schlecht, G. Chattopadhyay, F. Maiwald, N.R. Erickson, and I. Mehdi, IEEE Microwave and Wireless Components Lett., 14, 253 (2004).
3. D. Streit, R. Lai, A. Oki, A. Gutierrez-Aitken, 14th Indium Phosphide and Related Materials Conf., 11 (2002).
4. B. Jalali and S. Pearton, *InP HBTs Growth, Processing, and Applications*, Artech House Inc., Boston (1995).
5. D. Yu, K. Choi, K. Lee, B. Kim, H. Zhu, K. Vargason, J.M. Kuo, P. Pinsukanjana, and Y.C. Kao, IEDM Tech. Digest, 557 (2004).
6. W. Hafez and M. Feng, Appl. Phys. Lett., 86, 152101 (2005).
7. Z. Griffith, M. Dahlstrom, M.J.W. Rodwell, X.-M. Fang, D. Lubyshev, Y. Wu, J.M. Fastenau, W.K. Liu, IEEE Electron Device Lett., 26, 11 (2005).
8. Z. Griffith, M. Dahlstrom, M.J.W. Rodwell, M. Urteaga, R. Pierson, P. Rowell, B. Brar, S. Lee, N. Nguyen, C. Nguyen, Proc. Bipolar/BiCMOS Circuits and Tech., 176 (2004).
9. G. He, J. Howard, M. Le, P. Partyka, B. Li, G. Kim, R. Hess, R. Bryie, R. Lee, S. Rustomji, J. Pepper, M. Kail, M. Helix, R.B. Elder, D.S. Jansen, N.E. Harff, J.F. Prairie, E.S. Daniel, and B.K. Gilbert, IEEE Electron Device Lett., 25, 520 (2004).
10. K. Kurishima, S. Yamahata, H. Nakajima, H. Ito, and N. Watanabe, IEEE Electron Device Lett., 19, 303 (1998).
11. A. Fung, L. Samoska, J. Velebir, P. Siegel, M. Rodwell, V. Paidi, Z. Griffith, M. Urteaga, and R. Malik, Proc. 15th International Symposium on Space TeraHertz Technology, 323 (2004).

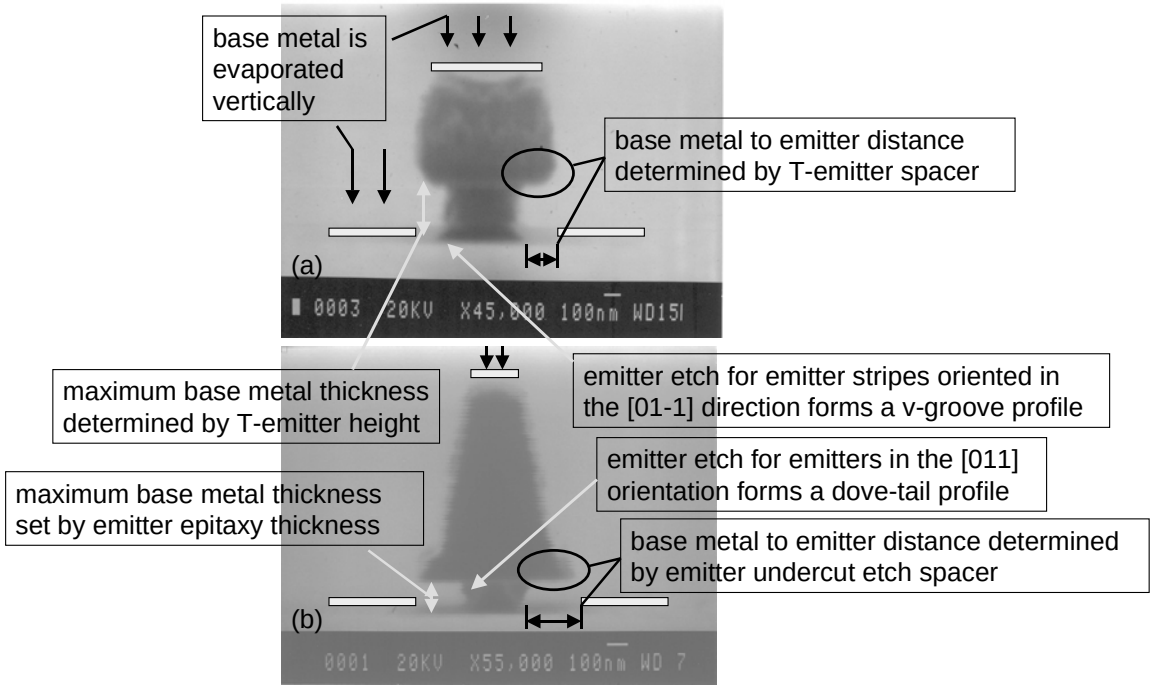

Figure 1. Scanning electron microscopy photos of profiles of emitter metal features after etching to the base layer. Base metal is drawn in for illustration. (a) T-emitter structure allows for more control of the base metal spacer distance and maximum base metal thickness through lithography. (b) In the conventional emitter structure the base metal spacer is set by the undercut etch, and the base metal height is fixed by the emitter epitaxy thickness.

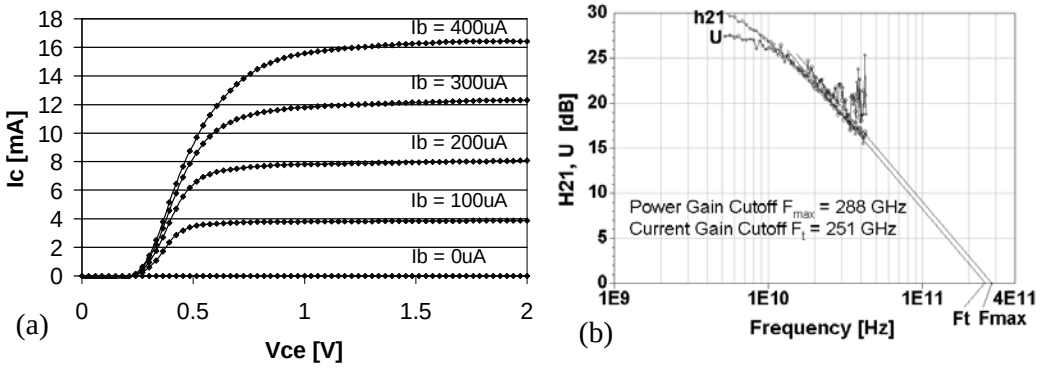

Figure 2. Electrical characteristics of a nominal 0.3x9 um^2 emitter stripe DHBT in the common emitter configuration. (a) Collector current versus collector-emitter voltage for different base currents. Small signal gain β is ~40 at Vce of 2V and Ic of 12 mA. (b) Mason's unilateral gain (U) and current gain (H21) calculated from measured RF S-parameters as a function of frequency. Extrapolated power gain cutoff frequency F_{max} is 288 GHz and current gain cutoff F_t is 251 GHz. DC bias conditions are Vce = 2.01V, Ic = 14.97mA, Vbe = 0.985V, Ib = 396.5uA.

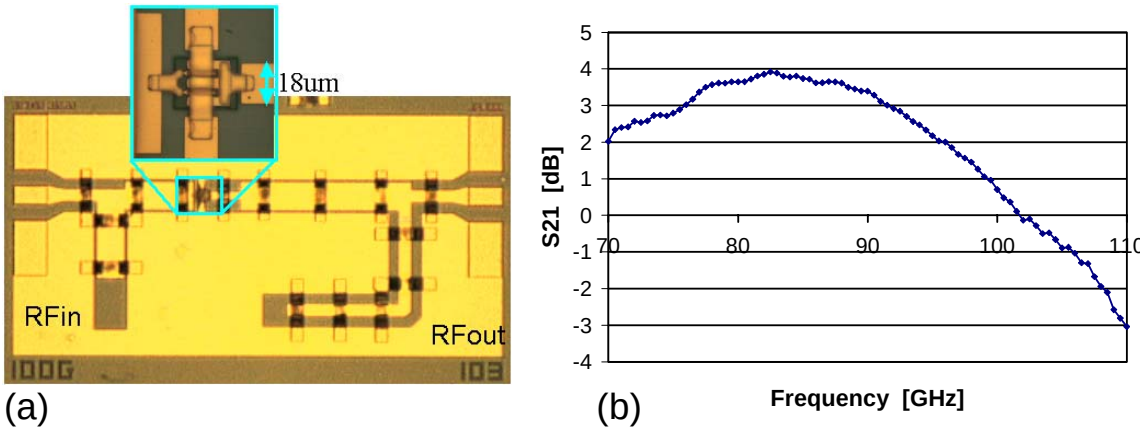

Figure 3. W-band MMIC amplifier results. (a) Optical photo of a dual 0.7umx12um emitter DHBT matched amplifier. (b) Amplifier S21 gain versus frequency. Gain is peaked at 82.5 GHz at 3.9 dB.